NASA CR-147770

MCDONNELL DOUGLAS TECHNICAL SERVICES CO.
HOUSTON ASTRONAUTICS DIVISION

(NASA-CR-147770) ANALYSIS OF EFFECT OF INTERNAL AND OPERATING VARIABLES ON PERFORMANCE OF SVDS CONSTRAINT MODEL (ABIND) (MCDONNELL-DOUGLAS TECHNICAL SERVICES) 35 P HC $4.00 CSCL 22B

SPACE SHUTTLE ENGINEERING AND OPERATIONS SUPPORT

DESIGN NOTE NO. 1.2-DN-B0205-10

# ANALYSIS OF EFFECT OF INTERNAL AND OPERATING VARIABLES ON PERFORMANCE OF SVDS CONSTRAINT MODEL (ABIND)

N76-25335

UNCLAS
G3/18 43521

ENGINEERING SYSTEMS ANALYSIS

26 JUNE 1975

This Design Note is Submitted to NASA Under Task Order No. B0205, Subtask 5, Task Assignment Flight Performance in Fulfillment of Contract NAS 9-13970

PREPARED BY: James R Pendergrass
J. R. Pendergrass
Associate Engineer
488-5660, Ext. 227

PREPARED BY: R. L. Walsh
R. L. Walsh
Task Manager
Separation Systems Performance
488-5660, Ext. 227

APPROVED BY: J. C. Weitekamp
J. C. Weitekamp
Technical Manager
Flight Performance
488-5660, Ext. 232

APPROVED BY: Robert Stephens
R. R. Stephens
Project Manager
Engineering Systems Analysis
488-5660, Ext. 204

## 1.0 SUMMARY

An examination of the factors which modify the simulation of a constraint in the motion of the aft attach points of the Orbiter and External Tank during separation has been made. The factors considered were both internal (spring and damper constants) and external (friction coefficient and dynamic pressure). The results of this study show that an acceptable choice of spring/damper constant combinations exist over the expected range of the external factors and that the choice is consistent with a practical integration interval. This constraint model is also shown to produce about a 10% increase in the relative body pitch angles over the unconstrained case whereas the MDC-STL constraint model is shown to produce about a 38% increase.

## 2.0 INTRODUCTION

A constraint model was developed by TRW for use in the Space Vehicle Dynamics Simulation (SVDS) program to provide a simulation of the binding characteristics of the ball and socket associated with the aft attach points of the Orbiter/External Tank during separation. This model, which is called ABIND, uses a spring-damper-mass system to model the force and moment interactions in the ball and socket. These interactions, which occur between the separating vehicles after release of the restraining mechanisms but before actual loss of physical contact must then be incorporated in to the equations of motion of each of the two bodies. As in all spring-damper-mass systems the force histories transmitted to the body masses are a function of the spring stiffness and damping used in the

simulation and the choice of spring and damper constants becomes representative of the quality of the simulation. This study will show the relationship between the choice of spring/ damper constants and the corresponding responses to them for a range of probable operating conditions. The primary operating conditions include the friction coefficient between the aft ball and socket and the dynamic pressure at separation. A comparison with an unconstrained simulation and an alternate constraint model are also briefly examined.

## 3.0 DISCUSSION

The ABIND constraint model provides a simulation of the components of the normal and frictional forces and torques that are developed within the ball and socket of the two aft attach points. This simulation uses a spring-damper-mass system to provide the force and torque components, but a tuning of the system is required to select the proper spring and damper constants. This selection must consider the force and moment profiles generated by the motion, the integration interval required by the computer to convert one force cycle into motion, and the resultant motion of the center of the ball as it leaves the socket.

Integration Interval - The aft attach of the Orbiter and External Tank is modeled by a simple parallel spring-damper-mass system and is, therefore, amenable to a theoretical estimate of the integration interval. From the basic formulation of spring-mass

systems, the rotational frequency of the oscillating forces can be derived as:

$$P = \sqrt{\frac{2Kg(W_1 - W_2)}{W_1 W_2}} \qquad \text{(rad/sec)}$$

where $W_1$ = Weight of Orbiter (lb.)

$W_2$ = Weight of External Tank (lb.)

$K$ = Spring Constant (lb/ft.)

$g$ = Gravitational Acceleration (ft/sec$^2$)

The period (T) can then be found as:

$$T = \frac{2\pi}{P} \qquad \text{(sec.)}$$

The minimum number of points required to define the cyclic forces in a 4th order Runge-Kutta integration is estimated at six per period. Thus, the maximum integration interval ($\Delta t$) is then found to be:

$$\Delta t = \frac{T}{6} = \frac{\pi}{3}\sqrt{\frac{W_1 W_2}{2Kg(W_1 - W_2)}} \qquad \text{(sec.)}$$

As shown in Figure 1 a spring constant no greater than $2.08 \times 10^7$ lb/ft. can be used with a maximum integration interval of .01 seconds for tank weights exceeding 80,000 lbs.

As an example, a safe comparison of an actual spring constant-integration interval relationship was explored by comparing the accuracy of a $\Delta t$ of .01 and .002 seconds for a typical spring constant of $10^6$ lb/ft. These results, which are presented in

Figure 2 shows that there is a very close match in the torques of the External Tank during separation. Even better results are obtained by comparing the integrated trajectory of the initial x-z motion of the ball in the socket, as in Figure 3. Thus, an integration interval of .01 seconds is capable of accurately following the dynamics corresponding to a spring constant of $10^6$ lb/ft.

Typical Data - Having selected an integration interval of .01 seconds, a typical data set can now be provided to describe the force, torque and trajectory outputs for an arbitrary input. This input uses the $10^6$ lb/ft. spring constant along with a damper constant (C) of $10^5$ lb-sec/ft, a friction coefficient ($\mu$) of .2 and a dynamic pressure ($\bar{q}$) of 10 lbs/ft$^2$. Other intial conditions and mass properties which are used throughout the study are contained in Table 1.

Figure 4 shows the Orbiter reaction force profiles for both the left and right attach points. It is apparent that the out-of-plane initial conditions cause the left attach to separate about .2 seconds before the right. It also shows that the axial force is far larger than either the vertical or lateral forces and that none of the force histories have any significant oscillations.

The torques about the x, y, z axes thru the Orbiter center-of-gravity are shown in Figure 5. This figure shows that the forces acting about the Orbiter c.g. produce significant torques

RLW 27 APR.'75

# ABIND ANALYSIS

THEORETICAL MAXIMUM ALLOWABLE INTEGRATION
INTERVAL FOR SPRING-MASS SIMULATION

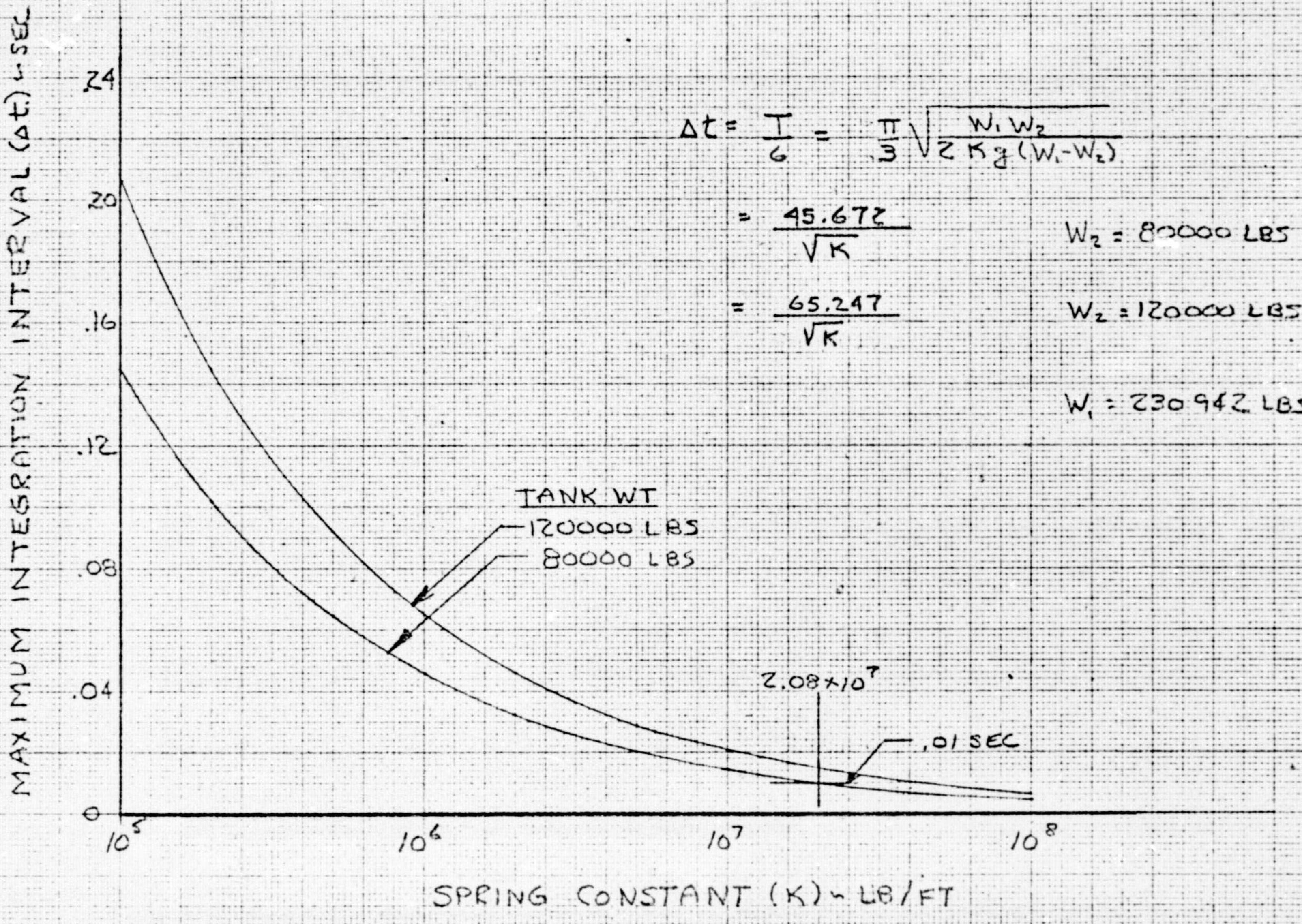


6

FIGURE 1

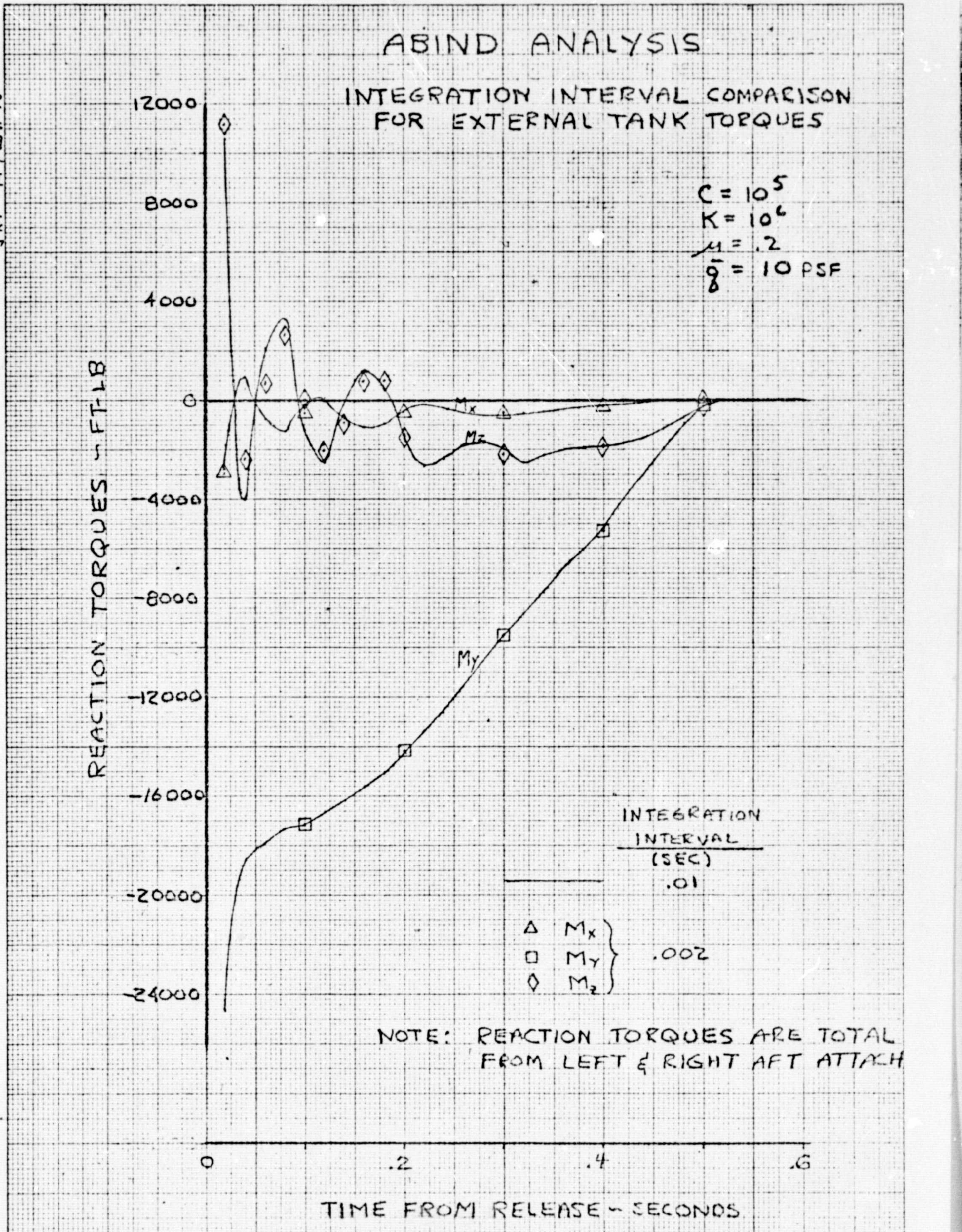
ABIND ANALYSIS
INTEGRATION INTERVAL COMPARISON FOR EXTERNAL TANK TORQUES
JRP 14 FEB. '75
C = 10^5
K = 10^6
μ = .2
q̄ = 10 PSF
REACTION TORQUES ~ FT-LB
12000
8000
4000
0
-4000
-8000
-12000
-16000
-20000
-24000
Mx
Mz
My
INTEGRATION INTERVAL (SEC)
.01
Δ Mx
□ My
◊ Mz
.002
NOTE: REACTION TORQUES ARE TOTAL FROM LEFT & RIGHT AFT ATTACH
0
.2
.4
.6
TIME FROM RELEASE ~ SECONDS



FIGURE 2

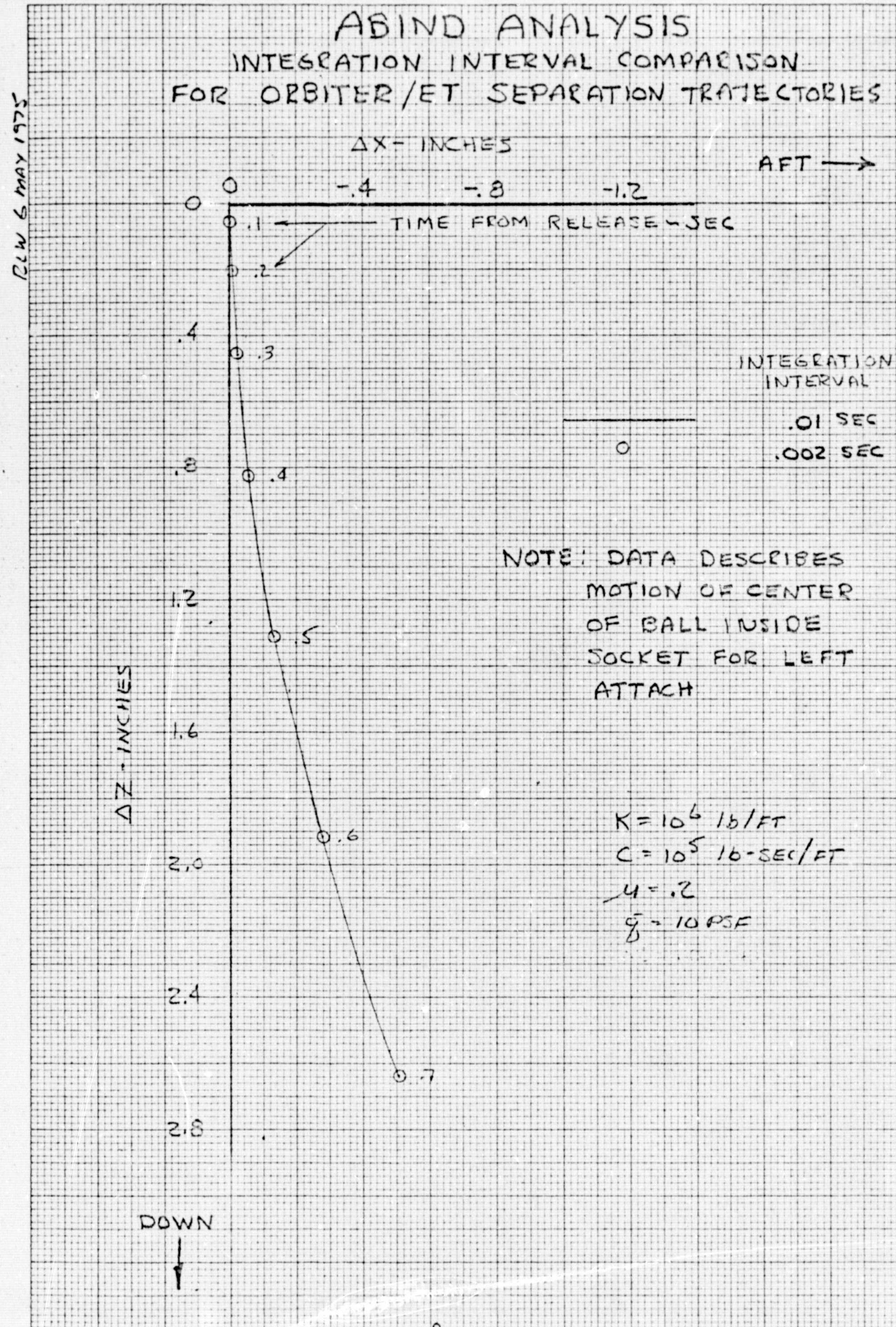
ABIND ANALYSIS
INTEGRATION INTERVAL COMPARISON
FOR ORBITER/ET SEPARATION TRAJECTORIES
RLW 6 MAY 1975
ΔX - INCHES
AFT →
0
-.4
-.8
-1.2
TIME FROM RELEASE - SEC
.1
.2
.3
.4
.5
.6
.7
ΔZ - INCHES
.4
.8
1.2
1.6
2.0
2.4
2.8
INTEGRATION INTERVAL
.01 SEC
.002 SEC
NOTE: DATA DESCRIBES MOTION OF CENTER OF BALL INSIDE SOCKET FOR LEFT ATTACH
K = 10^6 lb/FT
C = 10^5 lb-SEC/FT
μ = .2
q̄ = 10 PSF
DOWN



FIGURE 3

## ABIND ANALYSIS

## INTIAL CONDITIONS AND MASS PROPERTIES FOR STUDY

### INITIAL CONDITIONS*

$\alpha_i$ = -4 deg.

$\phi_i$ = $\beta_i$ = -0.5 deg.

$\dot{\Theta}_i$ = -0.25 deg/sec.

$\dot{\phi}_i$ = 0.5 deg/sec.

$\dot{\beta}_i$ = -0.5 deg/sec

$V_e$ = 6750 ft/sec.

$\psi_e$ = 90.0 deg.

| | | | |
|---|---|---|---|
| $\bar{q}$ | = 2 psf | 10 psf | 14 psf |
| h | = 245,105 ft. | 204,970 ft. | 195,927 ft. |

### MASS PROPERTIES

| | | ORBITER | TANK |
|---|---|---|---|
| Weight (lb.) | | 230942 | 80000 |
| CG Location (Inches) (in Vehicle Reference Coordinate System) | X | 1111.9 | 1363.2 |
| | Y | 0.6 | 2.0 |
| | Z | 380.6 | 418.5 |
| Inertias ($10^6$ slug-ft$^2$) | $I_{xx}$ | 0.8378 | 0.396 |
| | $I_{yy}$ | 6.489 | 4.588 |
| | $I_{zz}$ | 6.70 | 4.556 |
| | $I_{xy}$ | 0.003635 | 0.0 |
| | $I_{xz}$ | 0.1615 | 0.0 |
| | $I_{yz}$ | 0.002196 | 0.0 |

*These initial conditions are identical with those provided MDTSCO-H by MDAC-STL for out-of-plane case II and IV dated 24 August 1974. Constraint model was used only for case IV.



TABLE 1

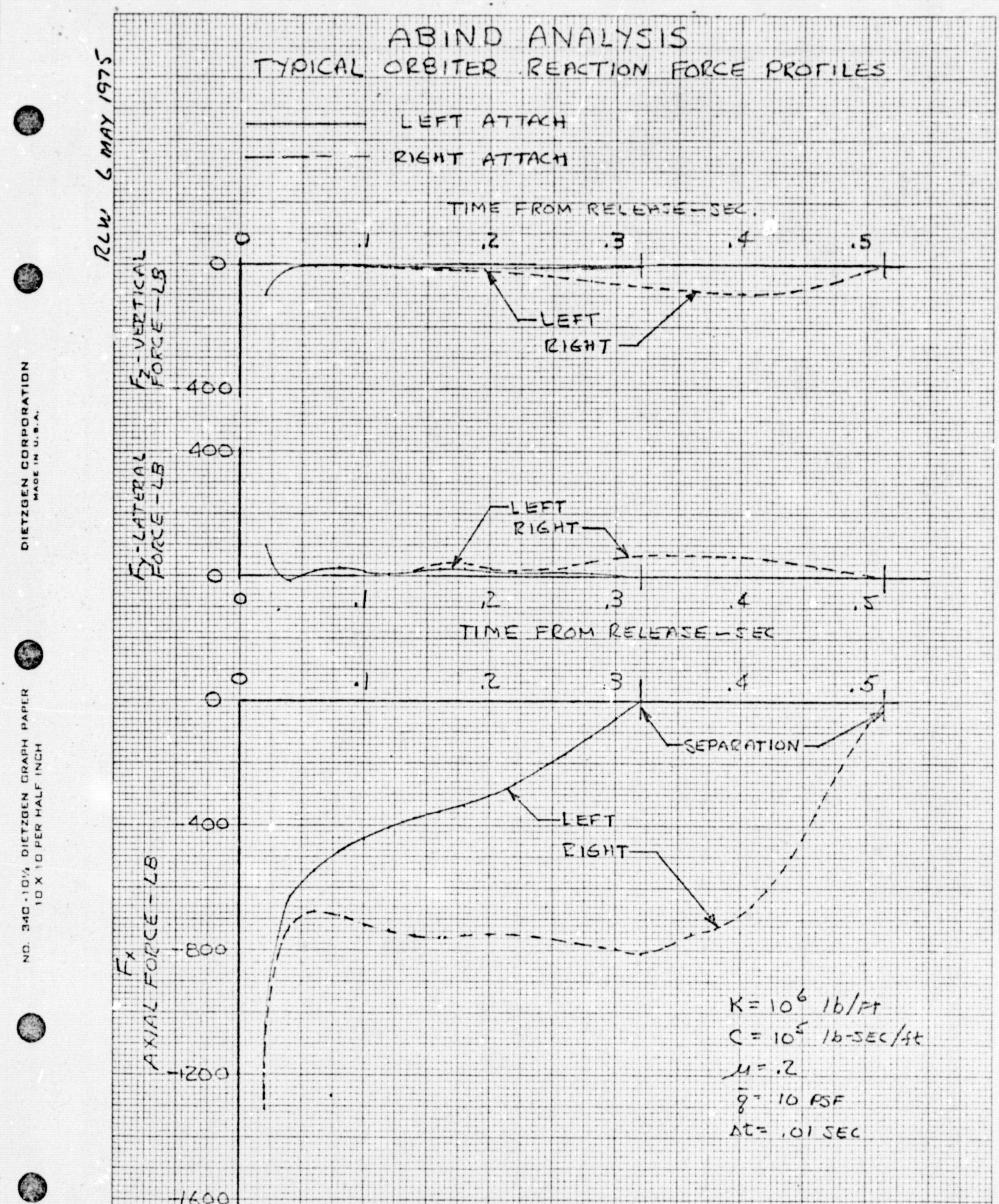

ABIND ANALYSIS
TYPICAL ORBITER REACTION FORCE PROFILES
LEFT ATTACH
RIGHT ATTACH
RLW 6 MAY 1975
TIME FROM RELEASE—SEC.
$F_z$-VERTICAL FORCE—LB
LEFT
RIGHT
$F_y$-LATERAL FORCE—LB
LEFT
RIGHT
TIME FROM RELEASE—SEC
$F_x$ AXIAL FORCE—LB
SEPARATION
LEFT
RIGHT
K = $10^6$ lb/ft
C = $10^5$ lb-SEC/ft
$\mu$ = .2
$\bar{q}$ = 10 PSF
$\Delta t$ = .01 SEC
DIETZGEN CORPORATION MADE IN U.S.A.
NO. 340-10½ DIETZGEN GRAPH PAPER 10 X 10 PER HALF INCH




FIGURE 4

# ABIND ANALYSIS

## TYPICAL ORBITER REACTION TORQUE PROFILES

RLW 6 MAY 1975

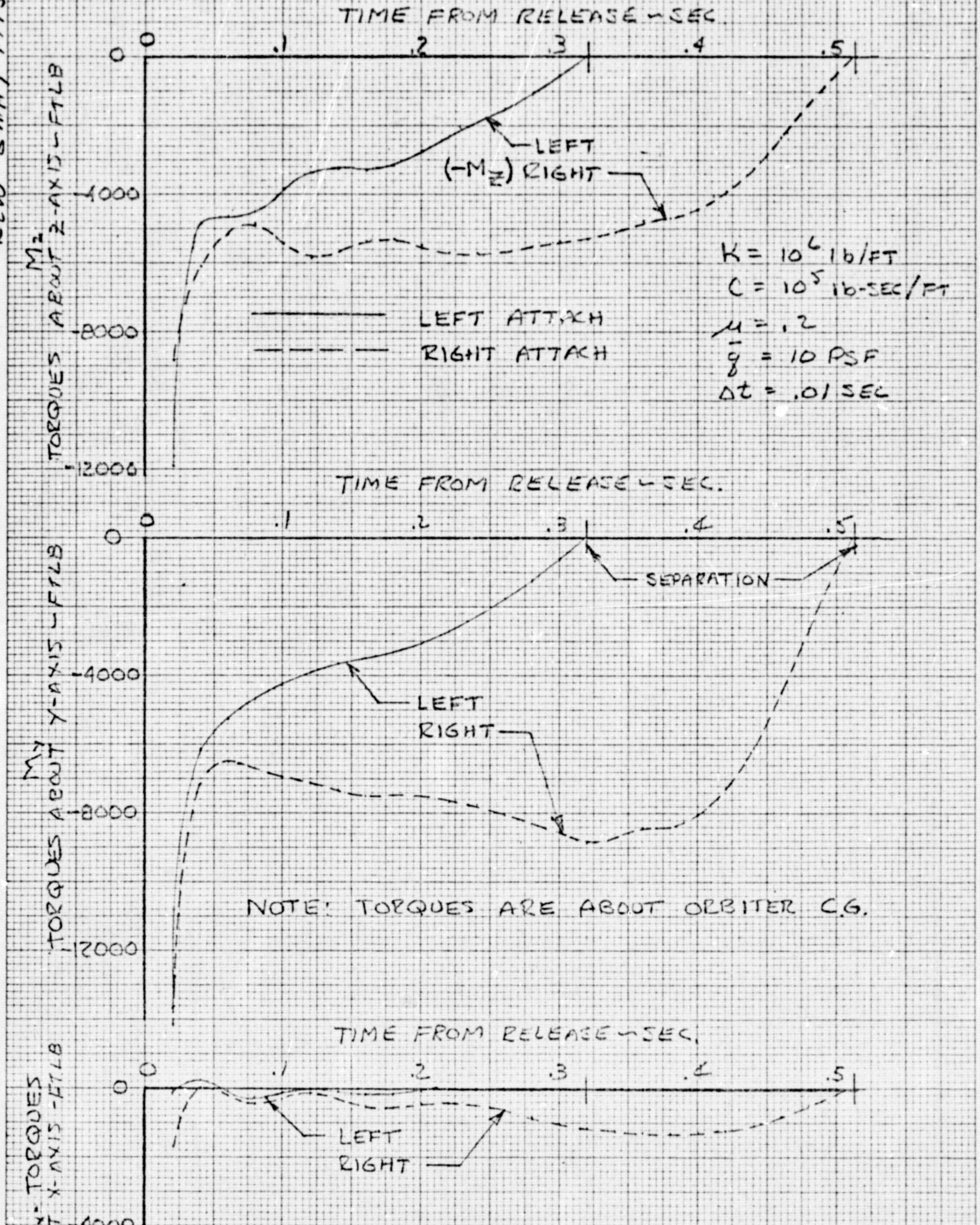






FIGURE 5

about the y and z axes. The torque profile about the y-axis (pitching torque) is similar in shape to the axial force profile although it also contains components of the vertical force in it. The torques about the z-axis (yawing torque) for each of the attach points are similar in shape but of opposite sign and hence tend to cancel each other whereas the pitching torques are additive. The torques about the x-axis (rolling torque) are very small by comparison. It can thus be shown that the single most significant reaction parameter for assessing spring/damper effectiveness can be demonstrated by the pitching torques.

The trajectories generated by the integration of the previously described forces and torques profiles are also indicative of the spring/damper constant response. Two types of trajectories are presented in Figure 6. The first shows the translation of the ball from the socket and the second shows the rotation of the ball as it is displaced vertically. These plots show that the left and right ball move in a very similar path for the first second of the trajectory. However, separation has occurred in less than 1.3 inches of vertical displacement and the deviation of the motion was determined by the forces and torques prior to separation.

Specific Objectives - Having examined the significant parameters which affect the determination of the spring/damper constants, the specific objectives of the study can now be identified. A matrix of spring and damper constants will be tested to

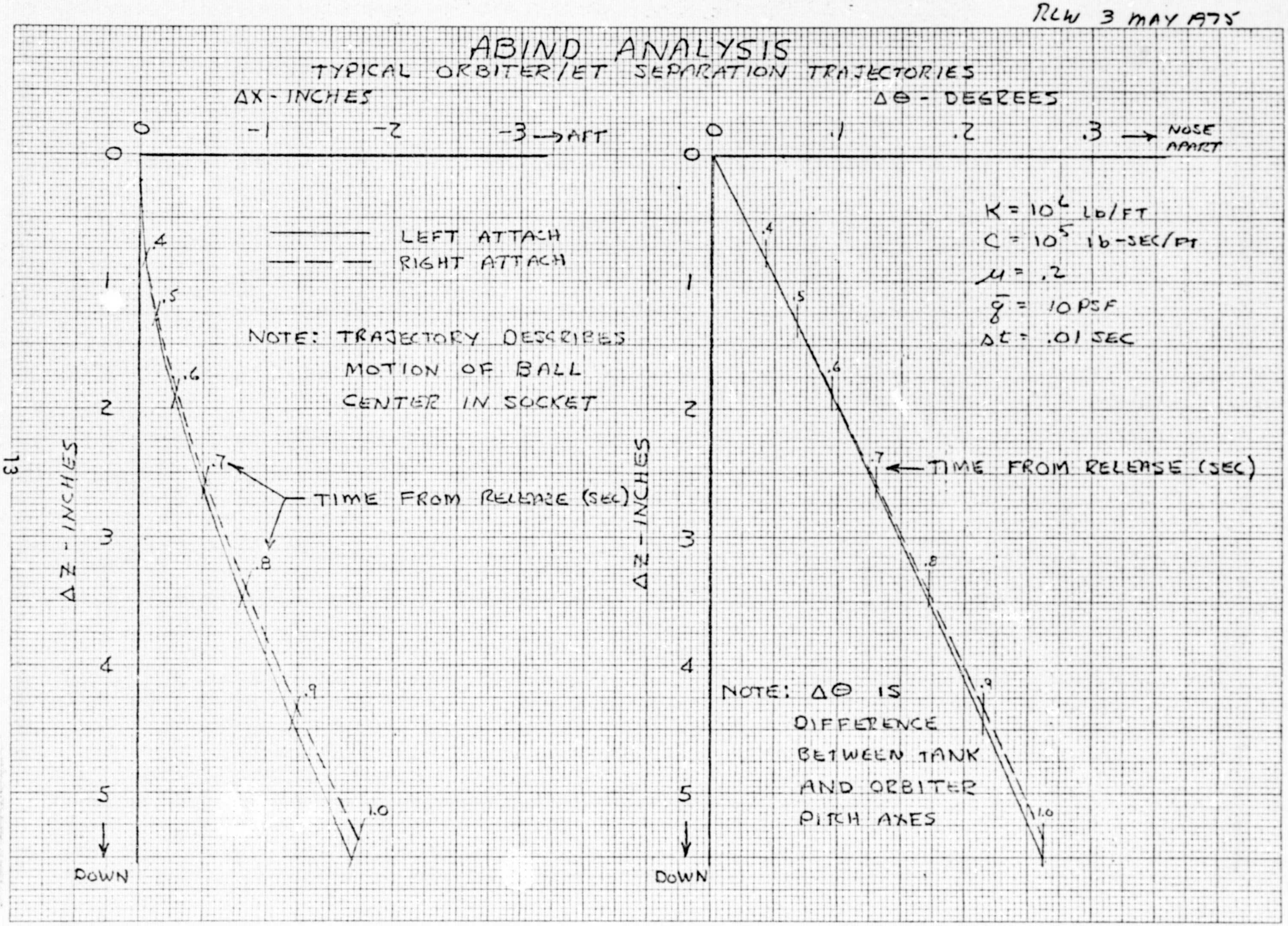
RLW 3 MAY 1975
ABIND ANALYSIS
TYPICAL ORBITER/ET SEPARATION TRAJECTORIES
ΔX - INCHES
0
-1
-2
-3 → AFT
LEFT ATTACH
RIGHT ATTACH
NOTE: TRAJECTORY DESCRIBES MOTION OF BALL CENTER IN SOCKET
TIME FROM RELEASE (SEC)
ΔZ - INCHES
1
2
3
4
5
DOWN
ΔΘ - DEGREES
.1
.2
.3 → NOSE APART
K = 10^6 lb/FT
C = 10^5 lb-SEC/FT
μ = .2
q̄ = 10 PSF
Δt = .01 SEC
NOTE: ΔΘ IS DIFFERENCE BETWEEN TANK AND ORBITER PITCH AXES
.4
.5
.6
.7
.8
.9
1.0



FIGURE 6

locate those combinations which produce non-dynamic pitching torque profiles. From this elimination procedure the criteria of trajectory deviation will be used to reduce the selection to a recommended set of spring/damper constants. The effects of dynamic pressure and friction coefficient will be determined and the results compared with similar trajectories determined with non-spring-damper-mass techniques and also with no active constraint model.

## 4.0 RESULTS

A selection of spring/damper constants was initiated by using the previously described data for $K = 10^6$ and $C = 10^5$ as a starting point. A matrix of other test conditions was established to locate the largest values that could be used in the simulation. As can be seen in Figure 7 some of the cases that failed were due to excessively large damper constants although acceptable spring constants were available. Theoretically, the failure of the $K = 10^8$ case was predicted by the data in Figure 1. The matrix was completed by producing nine cases which represented a 3x3 box of useable cases.

Pitching Torque Profiles - The pitching torque profiles from these nine cases are presented in Figures 8 and 9 for the left and right attach, respectively. The data are grouped by damper constants for each of the three spring constants. Both figures show similarities in the frequency of the oscillation but the right attach, which remained in contact longer, shows not only

R.I.W. 20 FEB. 75

# ABIND ANALYSIS

## SPRING/DAMPER CONSTANT MATRIX

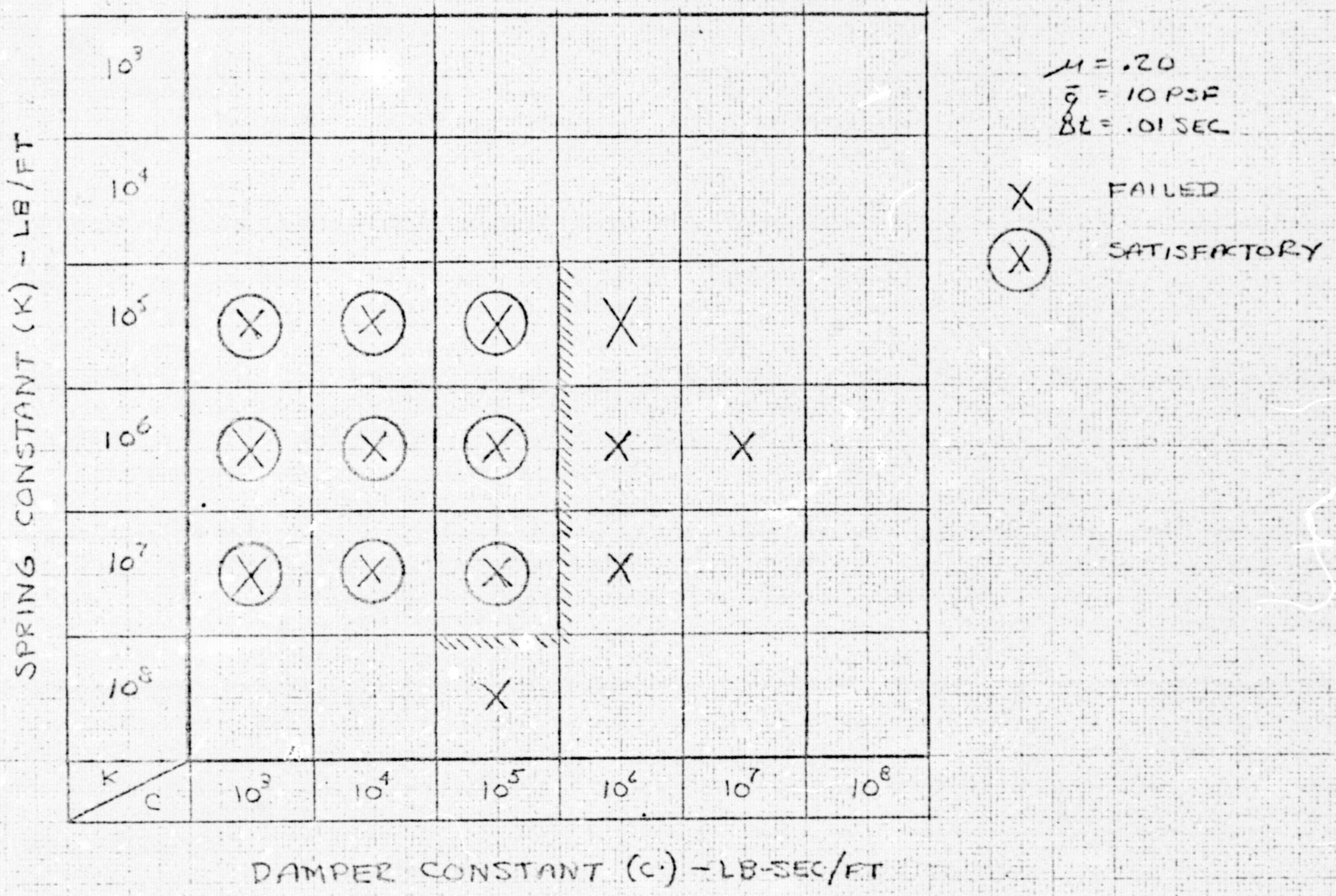




FIGURE 7

RLW 26 APR 75

# ABIND ANALYSIS

EFFECT OF SPRING/DAMPER CONSTANTS ON REACTION PITCHING TORQUES OF ORB/ET AFT ATTACH

LEFT ATTACH

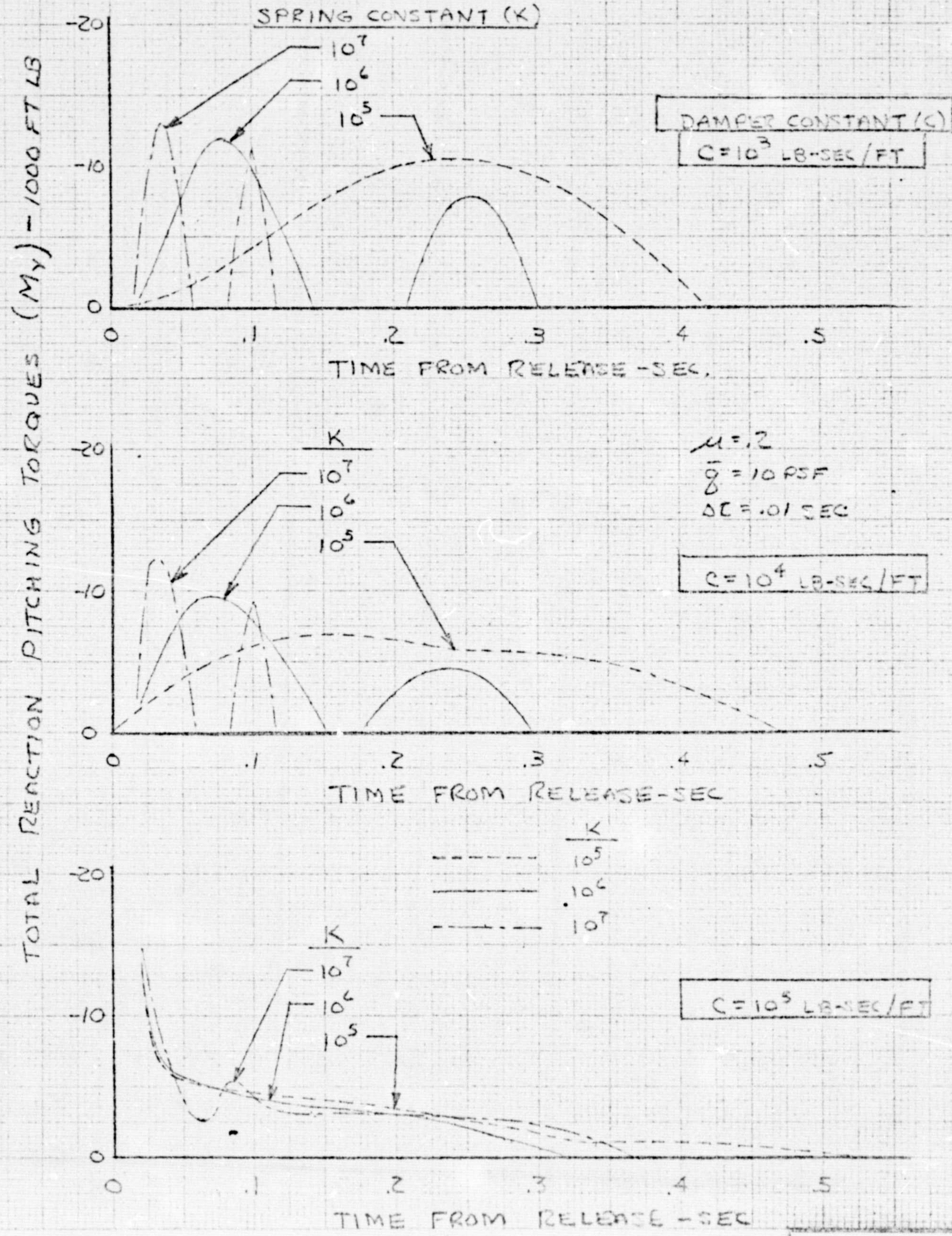




FIGURE 8

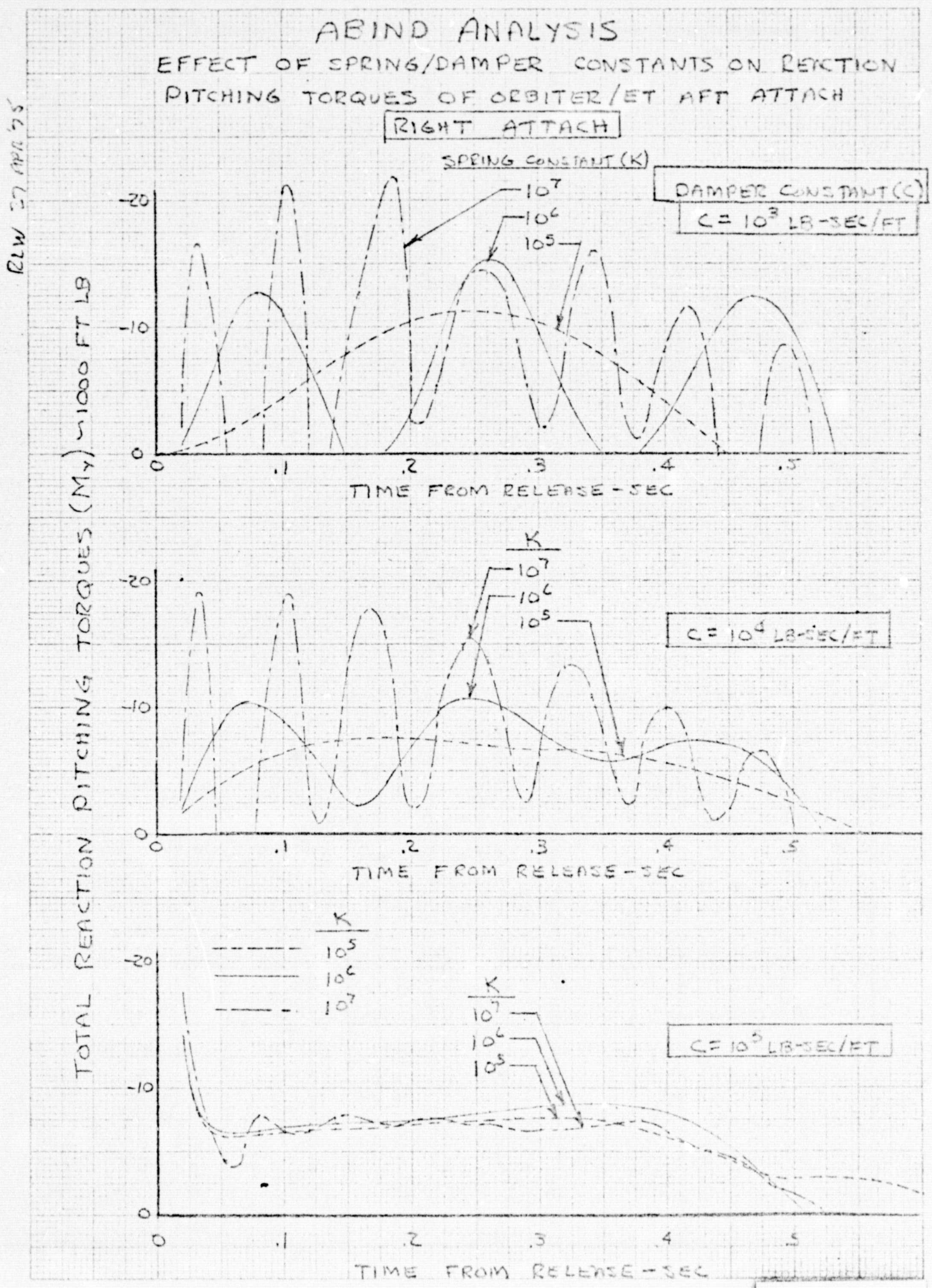

ABIND ANALYSIS
EFFECT OF SPRING/DAMPER CONSTANTS ON REACTION
PITCHING TORQUES OF ORBITER/ET AFT ATTACH
RIGHT ATTACH
RLW 27 APR '75
SPRING CONSTANT (K)
DAMPER CONSTANT (C)
C = 10^3 LB-SEC/FT
10^7
10^6
10^5
TOTAL REACTION PITCHING TORQUES (M_Y) ~ 1000 FT LB
TIME FROM RELEASE - SEC
K
C = 10^4 LB-SEC/FT
C = 10^5 LB-SEC/FT
-20
-10
0
.1
.2
.3
.4
.5




FIGURE 9

more oscillations but larger amplitudes. As can be seen in the figures, each of the subplots has a spring/damper constant combination which produces at least one non-dynamic torque profile. In the case of $C = 10^5$, only the pitching torques with $K = 10^7$ shows any indication of dynamics but the $K = 10^5$ case suggests a sluggishness to separate. Several of the curves "bottom out" indicating that the ball separated and rejoined the socket much like a bounce. The $C = 10^5$ data, unlike the others, shows a large initial spike in pitching torque which is quickly damped out.

Three of the nine cases are considered to have satisfied the criteria for non-dynamic pitching torque profiles while two others can be considered as close. A summary of these results is presented in Figure 10 where regions of degrees of acceptability and failure are constructed based on the test cases. This figure shows an acceptable region surrounded by a probably acceptable region. The selection of a suitable spring/damper constant combination should, therefore, be made from these two regions. Failure cases resulted from too large of an integration interval for the chosen constants.

All of the nine cases were made with typical conditions for dynamic pressure and friction coefficient of the ball and socket. The effect of varying these parameters was examined for the same constants of $K = 10^6$ and $C = 10^5$ and the matrix of these cases are presented in Figure 11. A range of dynamic

RLW 15 APR. '75

# ABIND ANALYSIS

EFFECT OF NON-DYNAMIC FORCE PROFILE CRITERIA ON SPRING/DAMPER

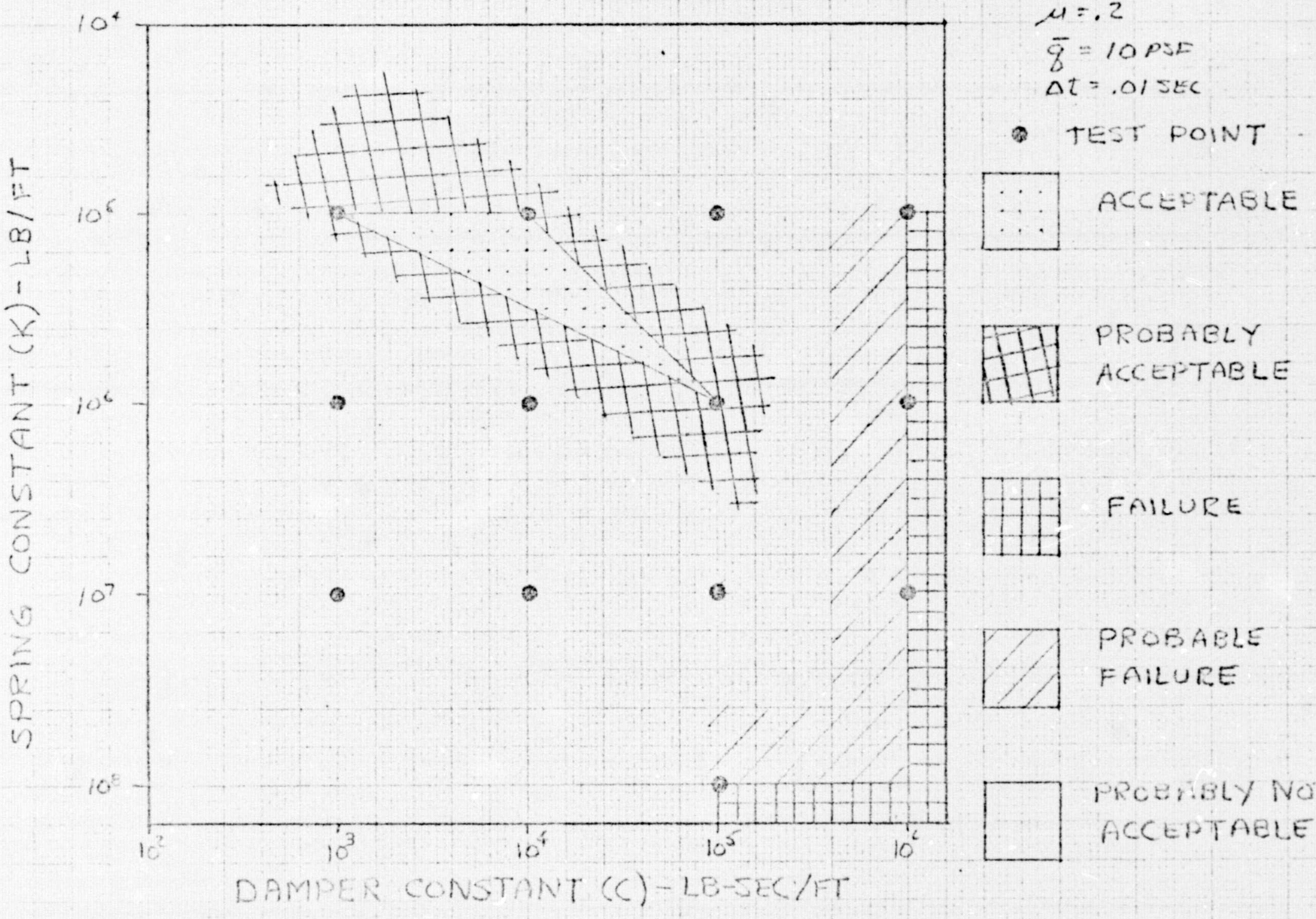


FIGURE 10

R.L.W. 28 FEB '75

# ABIND ANALYSIS

## DYNAMIC PRESSURE / FRICTION COEFFICIENT MATRIX

$C = 10^5$
$K = 10^6$
$\Delta t = .01$ SEC

DYNAMIC PRESSURE - PSF

FRICTION COEFFICIENT

| $\mu$ \ $\bar{q}$ | 2 | 10 | 14 |
|---|---|---|---|
| .1 | ⊗ | ⊗ | ⊗ |
| .2 | ⊗ | ⊗ | ⊗ |
| .3 | | ⊗ | |

X FAILED

⊗ SATISFACTORY



FIGURE 11

pressures from 2 psf to 14 psf and friction coefficients from .1 to .3 are included in this matrix. The pitching torque profiles for the range of dynamic pressures at $\mu = .2$ is presented in Figures 12 and 13 and although the absolute level of the data has changed (since portions of the forces are derived from air loads) the profile shape remains basically unchanged. A similar conclusion can be reached for variation in the friction coefficient which shows very little change. The largest difference occurs in the initial spike in the pitching torques as shown in Figures 14 and 15.

Trajectory Profiles - Although the pitching torque profiles can be used to narrow down the selection, the final choice must consider the integration of these profiles to produce acceptable displacement and rotation trajectories. The displacement trajectories for the center of the ball for the left and right attach are presented in Figues 16 and 17. These trajectories cover the first inch of travel which is just prior to final separation. These figures show that the trajectories for most of the constant combinations follow a path similar to the geometric track of axial displacement. Two obvious exceptions are for $K = 10^5$ at $C = 10^3$ and $10^4$ which are two of the three combinations which satisfies the pitching torque criteria. Only one of the three cases ($K = 10^6$ and $C = 10^5$) shows a close match in the displacements when compared with the expected geometric track which is shown on the right edge of the Figures

## ABIND ANALYSIS

## EFFECT OF DYNAMIC PRESSURE ON PITCHING TORQUES OF ORBITER / ET AFT ATTACH

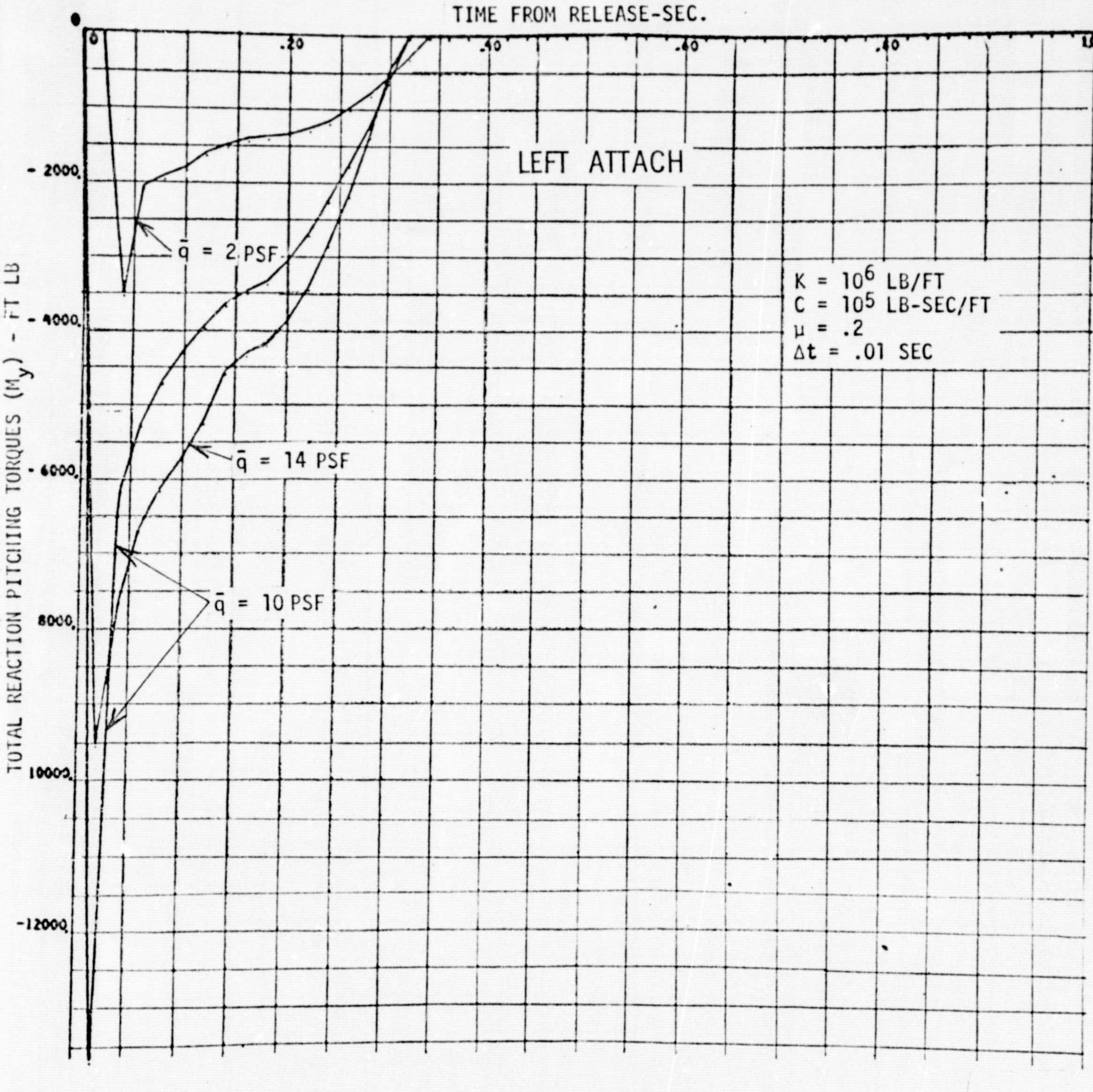




FIGURE 12

ABIND ANALYSIS

EFFECT OF DYNAMIC PRESSURE ON PITCHING TORQUES OF ORBITER / ET AFT ATTACH

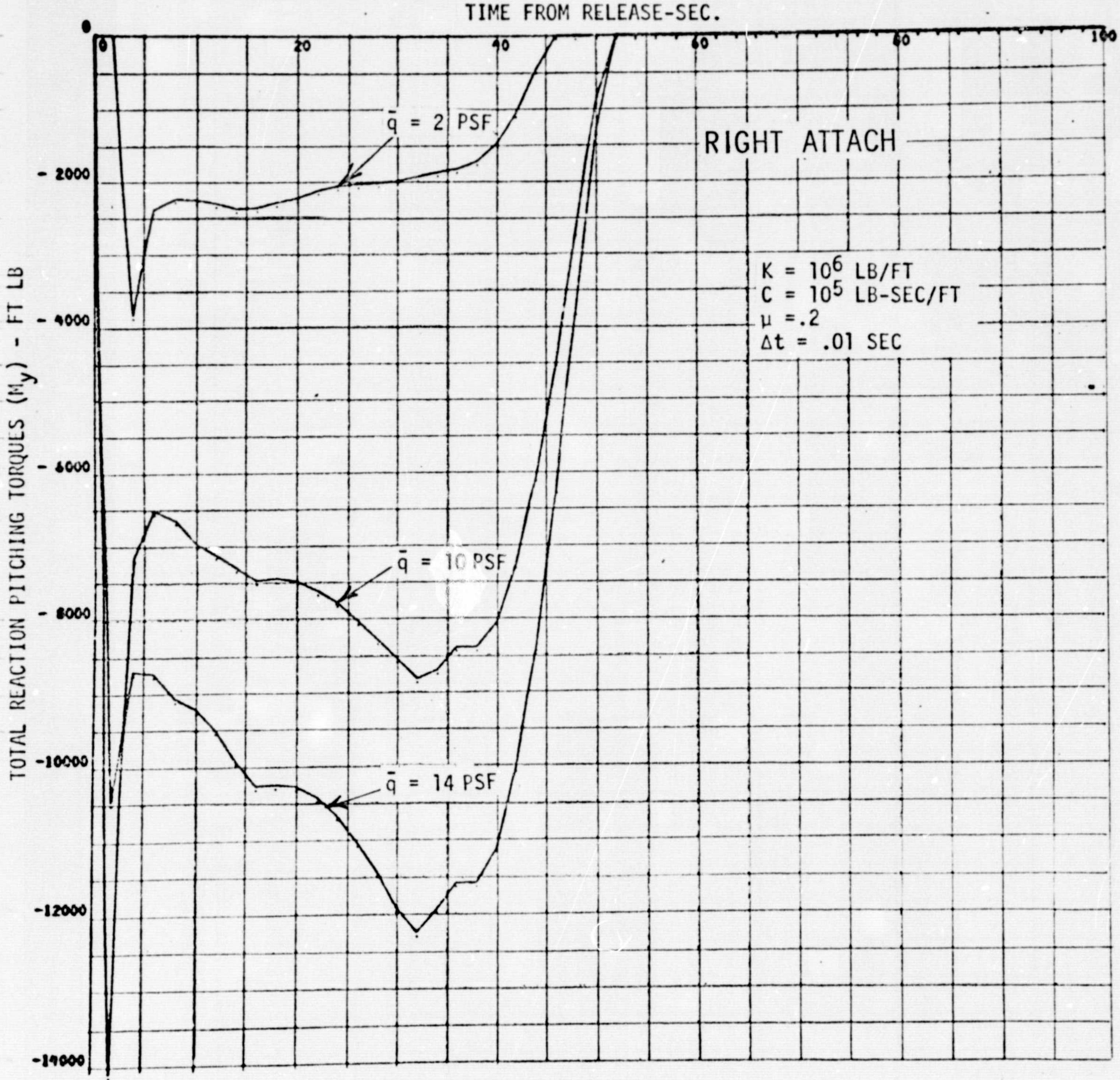




FIGURE 13

ABIND ANALYSIS

EFFECT OF FRICTION COEFFICIENT ON PITCHING TORQUES OF ORBITER/ET AFT ATTACH

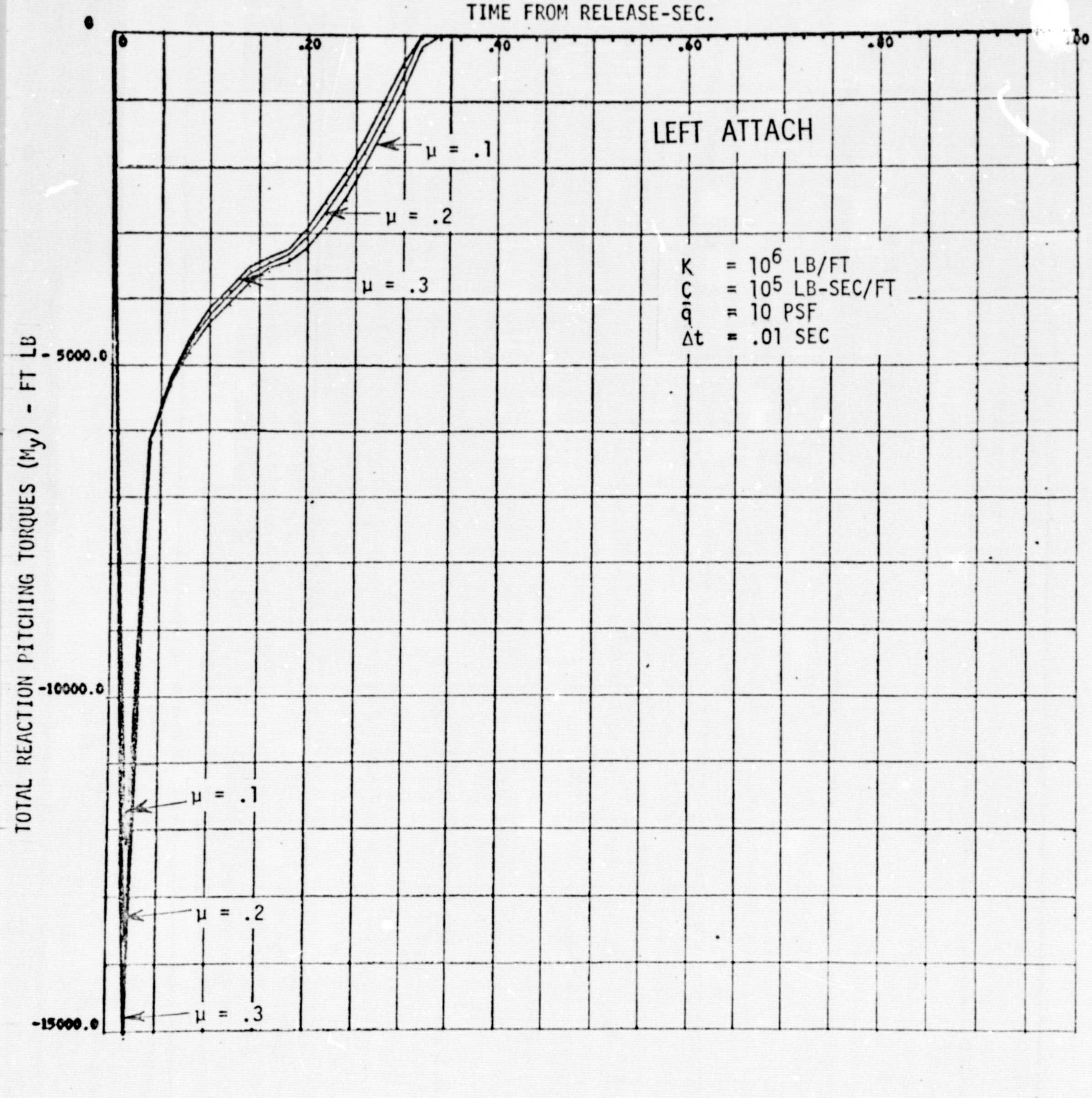




FIGURE 14

ABIND ANALYSIS

EFFECT OF FRICTION COEFFICIENT ON PITCHING TORQUES OF ORBITER/ET AFT ATTACH

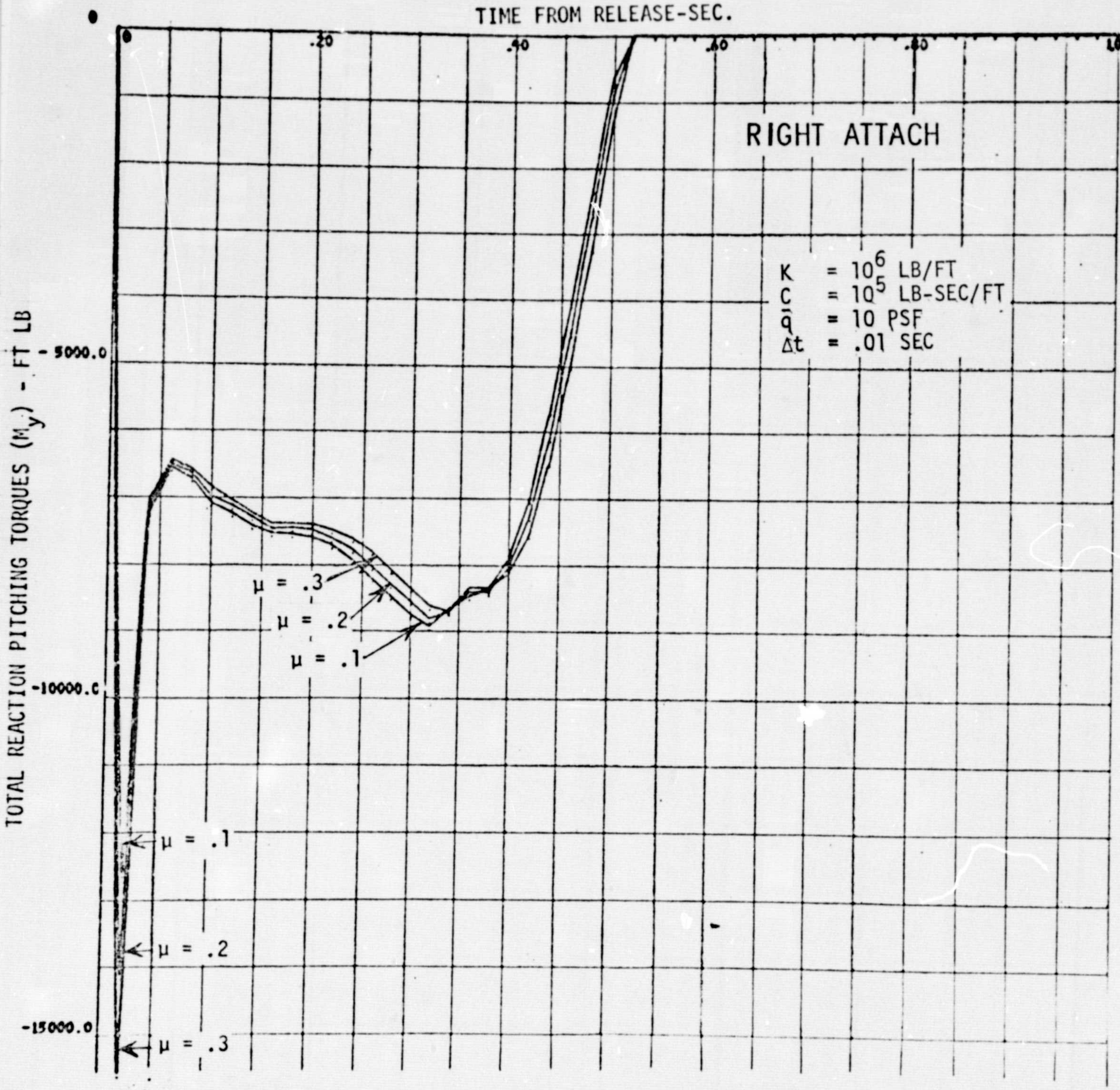




FIGURE 15

JRP 9 MAY 1975

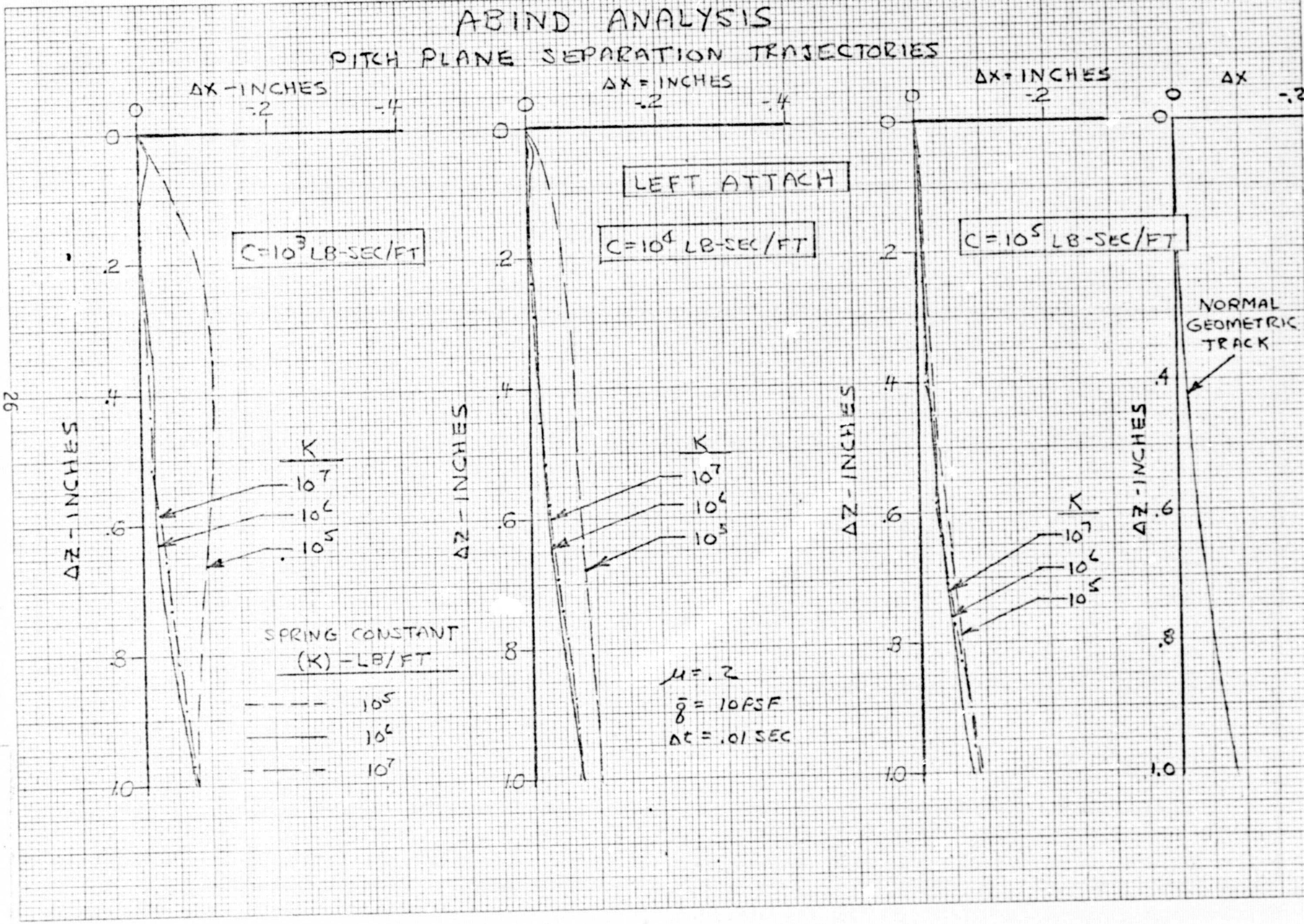




FIGURE 16

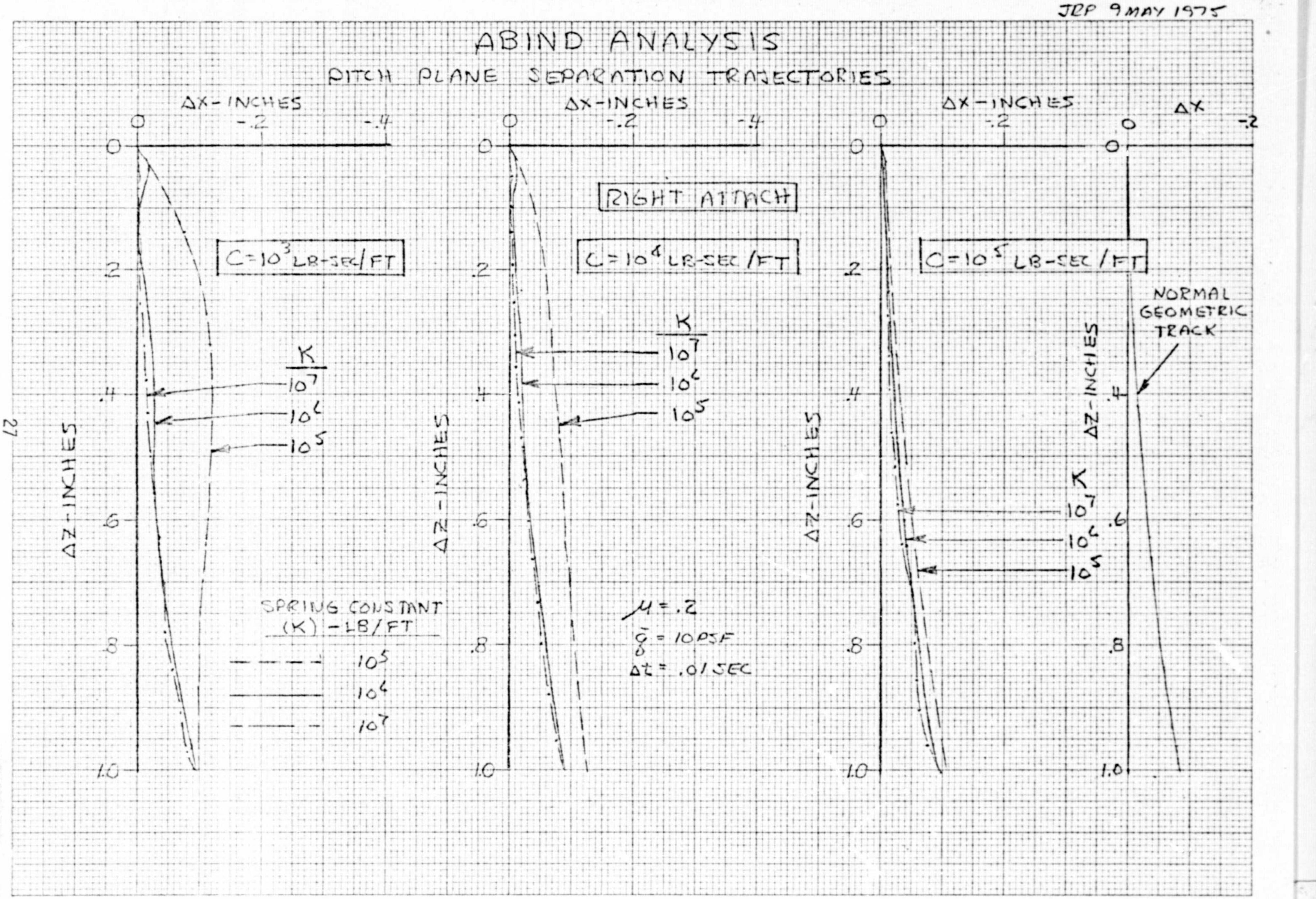
JRP 9 MAY 1975
ABIND ANALYSIS
PITCH PLANE SEPARATION TRAJECTORIES
ΔX-INCHES
ΔZ-INCHES
C=10³ LB-SEC/FT
C=10⁴ LB-SEC/FT
C=10⁵ LB-SEC/FT
RIGHT ATTACH
K
10⁷
10⁶
10⁵
NORMAL GEOMETRIC TRACK
ΔX
SPRING CONSTANT (K) - LB/FT
μ = .2
q̄ = 10 PSF
Δt = .01 SEC

FIGURE 17

16 and 17. The results from comparing the rotation trajectories is shown in Figure 18 for both the left and right attach. These curves show the relative insensitivity of this trajectory to the extremes of the nine spring/damper constant configurations during the first full second of the separation. This difference appears as a $\Delta\Theta$ error of about .015 degrees at the end of one second.

Constraint Model Comparisons - An evaluation of the ABIND constraint model with the other alternatives has been made in an earlier analysis (Reference 1). Additional comparisons are made here which emphasize the similarities and differences previously identified. These comparisons are made with the constrained and unconstrained simulations from the MDAC-STL program as well as the unconstrained simulation in SVDS and are presented in Figures 19 and 20. Figure 19, which presents the displacement trajectories of the ball center in the pitch plane, shows that the two constraint models follow a very similar path except for the time difference in reaching a given point. It also demonstrates one of the primary reasons for using a constraint model which is to simulate the restricted motion of the ball in the aft direction. This restriction shows as a reduction of about half of the axial displacement by the time the ball has left the socket ($\Delta Z$ = 6 inches).

Figure 20 presents a somewhat different conclusion as it shows that the constraint models produce more rotation and less vertical dis-

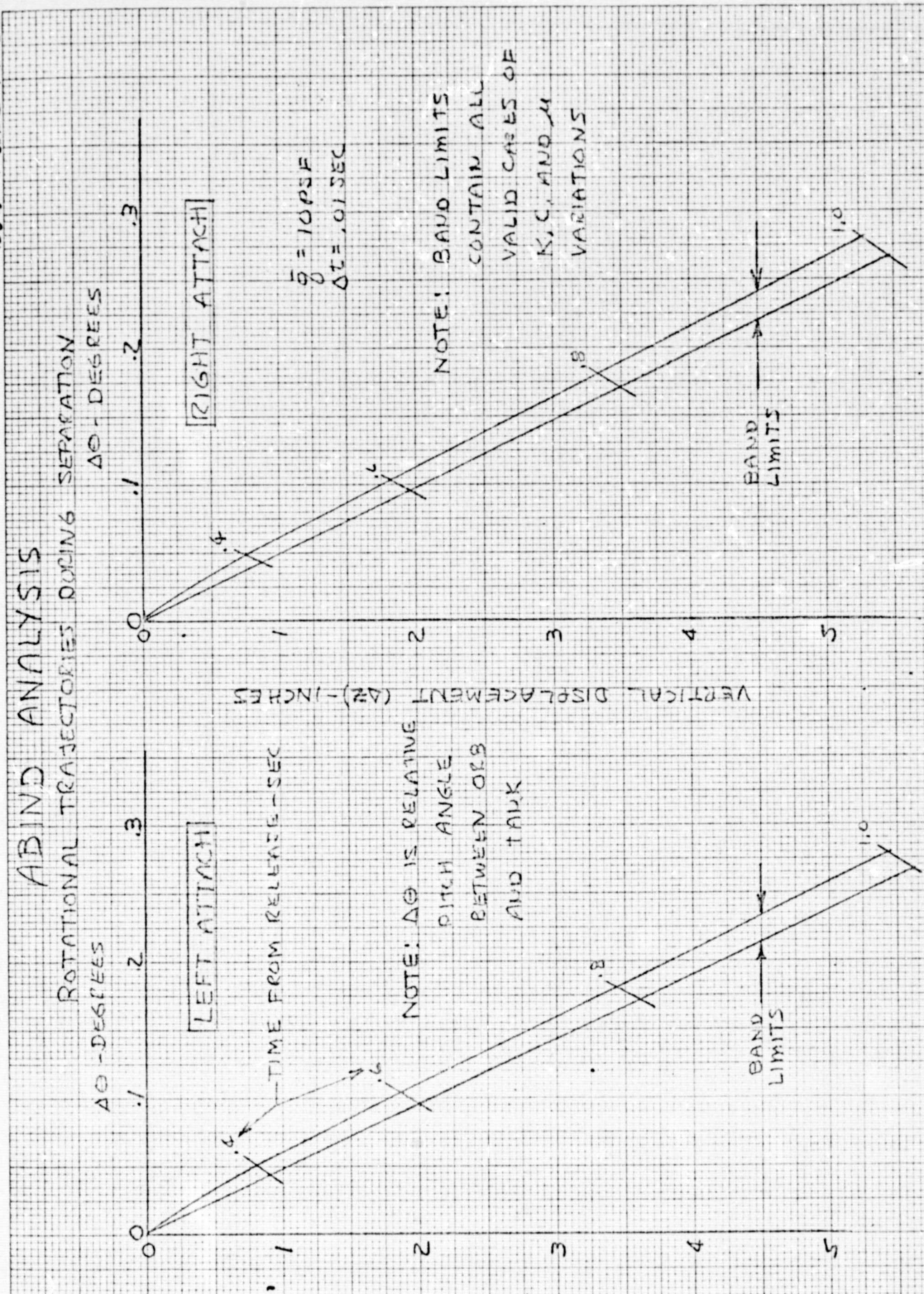
ABIND ANALYSIS
ROTATIONAL TRAJECTORIES DURING SEPARATION
RLW 4 JUNE 1975
LEFT ATTACH
Δθ - DEGREES
0
.1
.2
.3
TIME FROM RELEASE - SEC
.4
.6
.8
1.0
NOTE: Δθ IS RELATIVE PITCH ANGLE BETWEEN ORB AND TANK
BAND LIMITS
0
1
2
3
4
5
VERTICAL DISPLACEMENT (ΔZ) - INCHES
RIGHT ATTACH
Δθ - DEGREES
q̄ = 10PSF
Δt = .01SEC
NOTE! BAND LIMITS CONTAIN ALL VALID CASES OF K, C, AND μ VARIATIONS
.4
.6
.8
1.0
BAND LIMITS
0
1
2
3
4
5
VERTICAL DISPLACEMENT (ΔZ) - INCHES



FIGURE 18

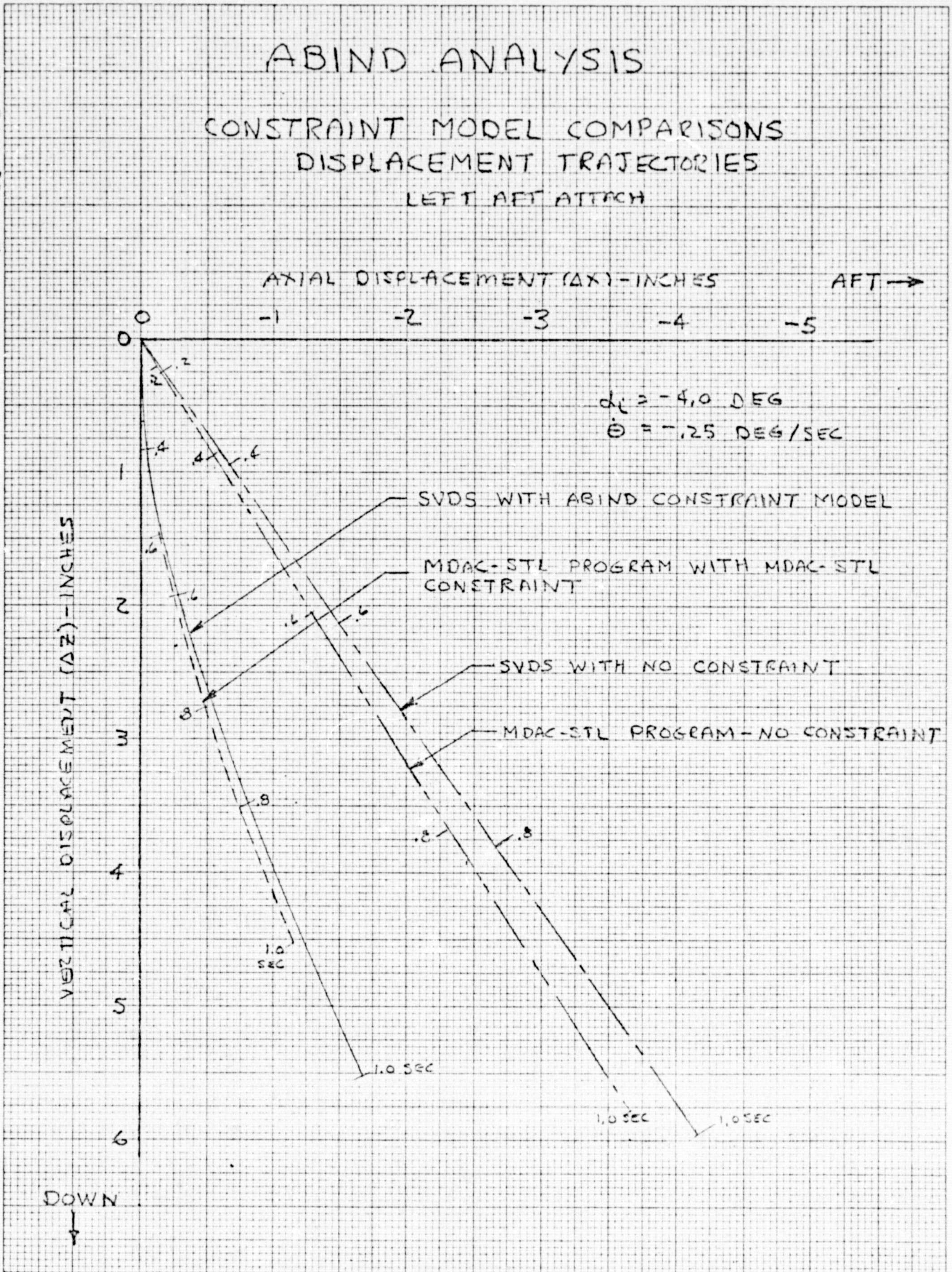
ABIND ANALYSIS
CONSTRAINT MODEL COMPARISONS
DISPLACEMENT TRAJECTORIES
LEFT AFT ATTACH
AXIAL DISPLACEMENT (ΔX) - INCHES
AFT →
0
-1
-2
-3
-4
-5
VERTICAL DISPLACEMENT (ΔZ) - INCHES
1
2
3
4
5
6
DOWN
αi = -4.0 DEG
θ̇ = -.25 DEG/SEC
SVDS WITH ABIND CONSTRAINT MODEL
MDAC-STL PROGRAM WITH MDAC-STL CONSTRAINT
SVDS WITH NO CONSTRAINT
MDAC-STL PROGRAM - NO CONSTRAINT
.2
.4
.6
.8
1.0 SEC




FIGURE 19

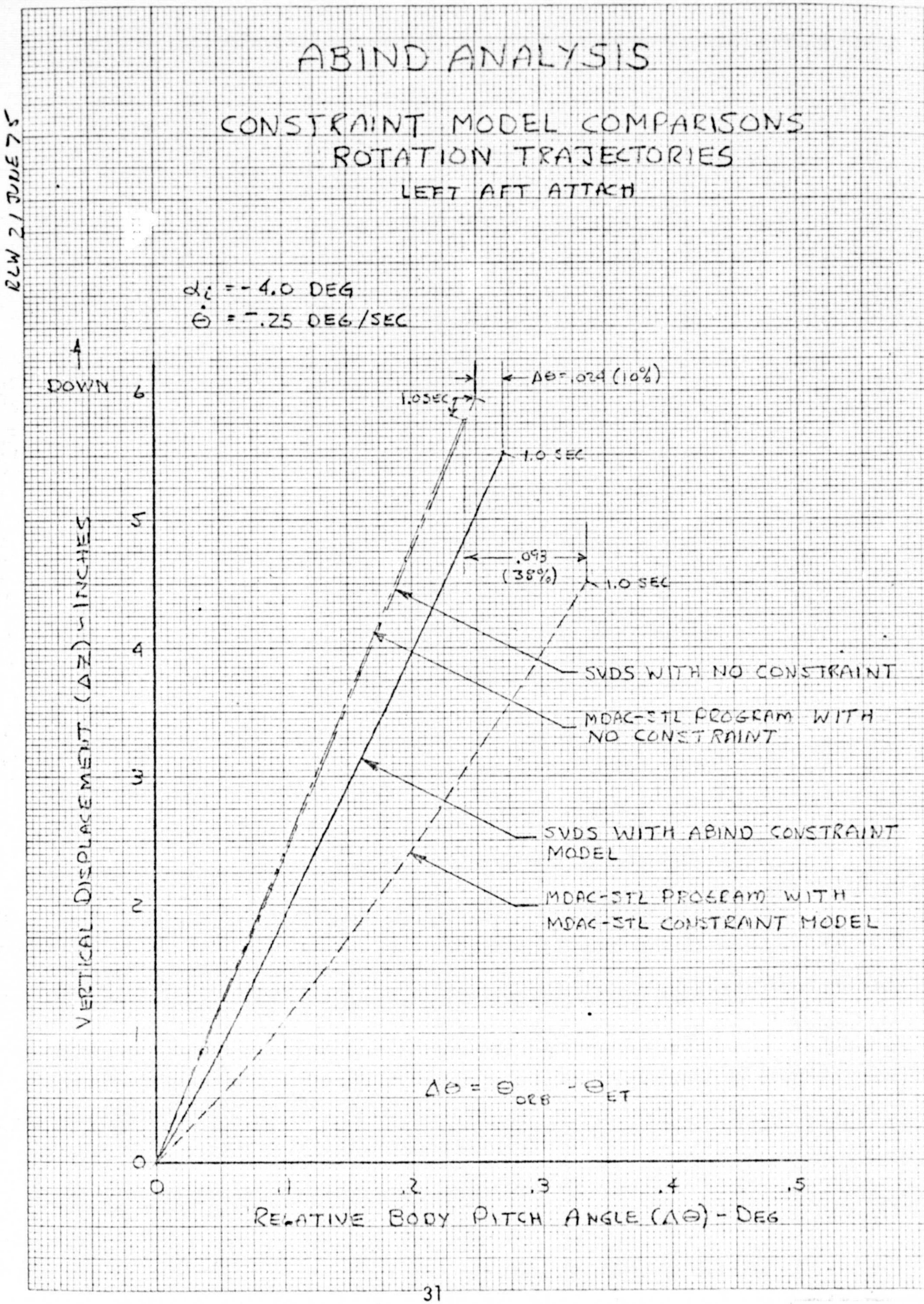

ABIND ANALYSIS
CONSTRAINT MODEL COMPARISONS
ROTATION TRAJECTORIES
LEFT AFT ATTACH
$\alpha_i$ = -4.0 DEG
$\dot{\Theta}$ = -.25 DEG/SEC
DOWN
$\Delta\Theta$=.024 (10%)
1.0 SEC
1.0 SEC
.093 (38%)
1.0 SEC
SVDS WITH NO CONSTRAINT
MDAC-STL PROGRAM WITH NO CONSTRAINT
SVDS WITH ABIND CONSTRAINT MODEL
MDAC-STL PROGRAM WITH MDAC-STL CONSTRAINT MODEL
$\Delta\Theta = \Theta_{ORB} - \Theta_{ET}$
VERTICAL DISPLACEMENT ($\Delta Z$) - INCHES
RELATIVE BODY PITCH ANGLE ($\Delta\Theta$) - DEG
0
1
2
3
4
5
6
0
.1
.2
.3
.4
.5
RLW 21 JUNE 75





FIGURE 20

placement than the unconstrained cases. This would be expected as the friction coefficient converts the potential energy of the vertical displacement into rotating the vehicles with respect to each other. The constraint model also changes the rotation center from the c.g. of each vehicle to the ball/socket attach point. However, more importantly, it shows that use of a constraint simulation produces nearly 4 times as much additional rotation with the MDAC-STL model ($\Delta\Theta$ = .093 degrees or 38%) than with the ABIND model ($\Delta\Theta$ = .024 degrees or 10%). This would indicate that one major difference between the constraint models is in the ability to convert potential energy to rotation. Were it not for the fact that the displacement trajectories produce the desired reduction in axial displacement there would be little advantage in using the ABIND constraint model in the SVDS program.

## 5.0 CONCLUSIONS

An examination of the factors which modify the simulation of binding in the aft attach points of the Orbiter and External Tank during separation has been completed. The factors considered were both internal (spring and damper constants) and external (friction coefficient and dynamic pressure). The criteria for the examination was based on an acceptable integration interval, a non-dynamic pitching torque-time history profile and a smooth displacement of the trajectories of the center of the ball as it rotates and translates out of the socket. As a result of these considerations the following conclusions can be stated:

1) An estimate of the maximum integration interval allowed in the study can be made using spring-mass dynamic analyses.
2) An integration interval of .01 seconds is acceptable for all springs with constants less than $2.08 \times 10^7$ lbs/ft for all tank weights exceeding 80,000 lbs.
3) Separation times for the left and right side are dependent on initial out-of-plane conditions. The right side is in contact longer for an Orbiter with a positive roll rate with respect to the Tank.
4) The torque profiles are similar for either aft attach point.
5) The pitching torque is the most significant parameter for assessing spring/damper effectiveness.
6) Based on analysis of the pitching torque time histories, only three of the test cases produce non-dynamic profiles.

7) Pitching torques show little sensitivity to variations of friction coefficients between .1 and .3.

8) Pitching torque profiles have different magnitudes but similar shape for dynamic pressures between 2 and 14 psf.

9) Only one of the three profile-acceptable test cases exhibited smooth displacements in the axial direction during separation.

10) All nine test cases produce only slight deviations in the rotation trajectories.

11) Only one of the nine test cases satisfies all of the established criteria ($K = 10^6$, $C = 10^5$).

12) Differences in displacement trajectories due to constraint model methods are small.

13) ABIND does not produce as severe a change in the rotational trajectories as the MDAC-STL constraint model.

14) A choice of spring/damper constants exist which allow ABIND to model the forces and torques at the aft attach points.

## 6.0 RECOMMENDATIONS

The analyses performed herein has demonstrated that differences between the MDAC-STL and SVDS constraint models exist. It is therefore recommended that a series of cases comparing the two different constraint simulation models with the unconstrained simulation be made using initial conditions near the former left hand boundary of the separation window. Comparison of these cases will indicate the sensitivity of the boundary to the constraint model.

## 7.0 REFERENCES

1. Subtask 5, Separation Systems Performance, MDAC-STL/SVDS Methodology Comparison Study for Unconstrained and Constrained Aft Attach Motion During RTLS External Tank Separation, 1.2-TM-B0105-164. 28 January 1975